

Independent 1D Nanosized Metal–Organic Tube: Anion Exchange, Separation, and Anion-Responsive Luminescence

Chao Fang, Qi-Kui Liu, Jian-Ping Ma, and Yu-Bin Dong*

College of Chemistry, Chemical Engineering and Materials Science, Key Laboratory of Molecular and Nano Probes, Engineering Research Center of Pesticide and Medicine Intermediate Clean Production, Ministry of Education, Shandong Provincial Key Laboratory of Clean Production of Fine Chemicals, Shandong Normal University, Jinan 250014, People's Republic of China

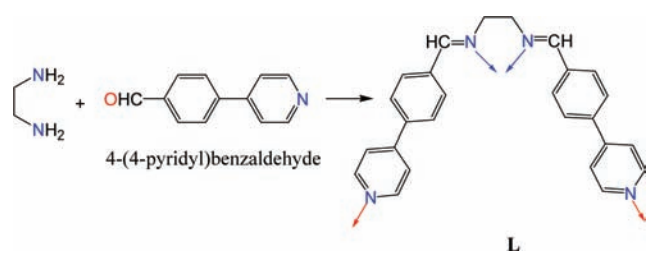
Supporting Information

ABSTRACT: Three independent 1D metal–organic nanotubes $\text{Ag}_2\text{L}_2\text{X}_2$ [$\text{X} = \text{PF}_6^-$ (1), ClO_4^- (2), and SbF_6^- (3)] with anion exchange, separation, and anion-responsive photoluminescence are reported.

Metal–organic frameworks (MOFs) have attracted significant attention because of their potential applications in gas storage, chemical separation, catalysis, and luminescence.¹ Despite numerous MOFs with tubular channels described in the literature,² however, reports of the independent 1D nanosized metal–organic tubes are quite rare to date.³ As we know, the construction of discrete 1D metal–organic nanotubes is very hard because of the inherent difficulty in the design and synthesis of the organic ligands with specific binding sites and orientations required by the tubular structures. On the other hand, a versatile metal coordination geometry is not easy to meet with the linking mode of the organic ligand to form a discrete 1D cylindrical structure.

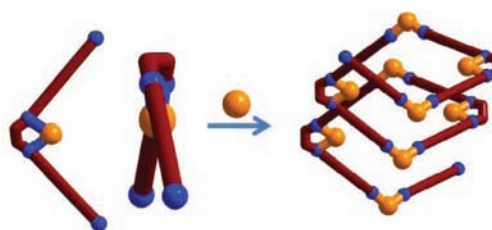
One of the promising approaches for the construction of independent 1D metal–organic nanotubes is to make use of metal–organic nanospirals. As we know, helical chains can form hollow, tube-shaped structures during their extension. The appropriate choice of organic spacers with specific geometry is a major factor in achieving helical chains and, furthermore, tubular structures. As shown in Scheme 1, the multifunctional

Scheme 1. Synthesis of L



double-Schiff-base ligand **L** was deliberately designed. It possesses a central chelating N,N site, which can bind to a metal ion to force itself into a cis conformation with a bent shape. In addition, the flexible $-\text{CH}_2\text{CH}_2-$ linker would induce two long phenylpyridine arms to be noncoplanar but twist. Such a scaffold is inclined to link metal nodes to form a helical array rather than a spherical one (Scheme 2).

Scheme 2. Formation of a Helical Chain Based on a Metal–Ion-Assisted Bent Organic Ligand



Depending on this approach, a series of independent 1D nanosized metal–organic tubes $\text{Ag}_2\text{L}_2\text{X}_2$ [$\text{X} = \text{PF}_6^-$ (1), ClO_4^- (2) and SbF_6^- (3)] are synthesized. X-ray crystal structure analysis (Supporting Information) revealed that 1–3 are isostructural and crystallize in the orthorhombic space group $Ccca$. For example, in 1, there are two crystallographically independent Ag^{I} centers, and they all lie in a distorted tetrahedral coordination sphere (Supporting Information). As shown in Figure 1, Ag^{I} ions are linked together by Ag^{I} -assisted

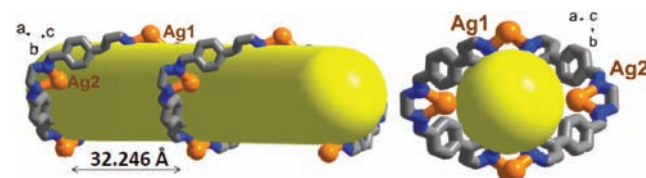


Figure 1. Side (left) and top (right) views of a 1D single-helical chain in 1.

bent ligand **L** into a 1D helical chain with a period of separation of ~ 32 Å.

Notably, each four-coordinate Ag^{I} ion serves as not only a node to bend the Schiff-base ligand but also a connector to extend the helical chain along the crystallographic c axis. Upon close inspection of the structure, there are two sets of helical strands in 1. Figure 2 shows that each strand consists of two individual one-handed helical chains that symmetrically surround the central axis to form an ellipselike tubular structure. Furthermore, two sets of strands intertwine each other and are interlocked by a $\{\text{AgN}_2\}$ linkage to eventually form a squarelike nanotube. The open channel of $\sim 1.1 \times 1.1$

Received: August 14, 2011

Published: March 22, 2012

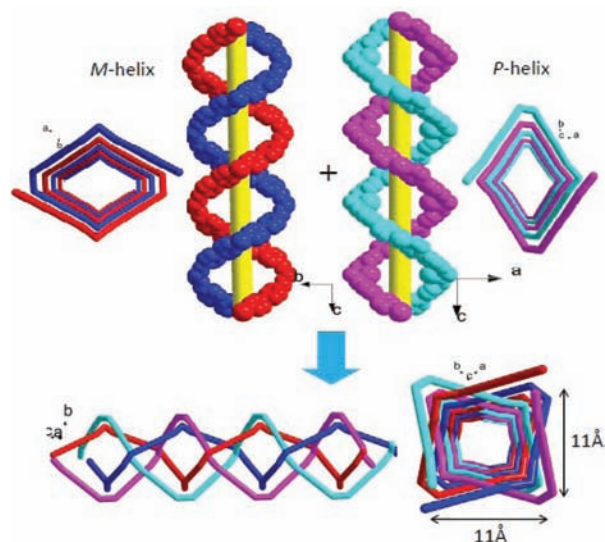


Figure 2. Left- and right-handed strands consisting of a nanotube.

nm dimensions is filled with PF_6^- counterions and disordered MeOH molecules.

As shown in Figure 3, the P2F_6^- anion is weakly bound to the framework through two sets of C–H...F bonds. The

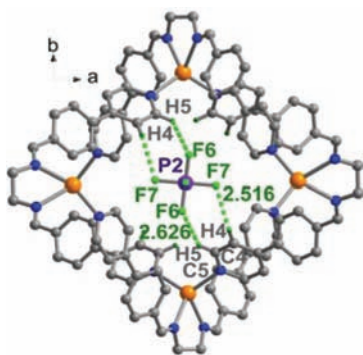


Figure 3. Encapsulated PF_6^- anion fixed by two sets of F...H hydrogen bonds in **1**. The encapsulated MeOH molecules have been removed for clarity.

hydrogen-bonding system involves the F atom of PF_6^- and the pyridyl H atom on the framework. The F6...C5 and F7...C4 distances are 3.257(5) and 3.294(5) Å, respectively. The corresponding F...H–C angles are 141 and 125°, respectively. In addition, the packing of adjacent tubes along the crystallographic c axis also leads to smaller open square channels of $\sim 6.6 \times 6.6$ Å that are occupied by the rest of the P1F_6^- anions (Figure 4). This is different from P2F_6^- in the tube; P1F_6^- is tightly bound by multiple F...H–C bonds (Supporting Information). Notably, the encapsulated MeOH guests can escape from the channel cavities at room temperature to generate the solvent-free Ag_2L_2 tube, which was confirmed by elemental analysis and thermogravimetric analysis (TGA; Figure 4). The powder X-ray diffraction (PXRD) patterns indicate that the framework of **1** remains intact upon removal of all MeOH molecules (Supporting Information).

Anion recognition and separation is currently a very active topic because various anions play central role in chemical and biological processes.⁴ The design of anion receptors, however,

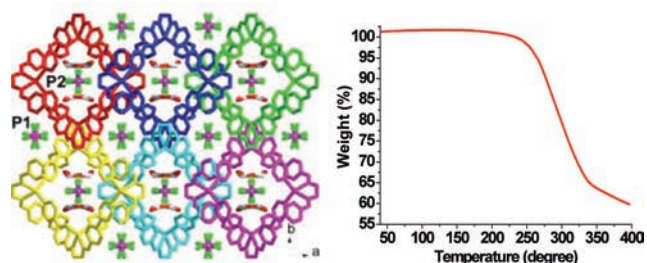


Figure 4. Left: Crystal packing of **1**. Right: TGA trace on a desolvated sample of **1**.

is challenging.⁵ As shown above, compounds **1–3** are cationic metal–organic tubes, and the counterions occupied the framework void and were uncoordinated to the metal centers. So, we wondered if the encapsulated anions could be exchanged by other kinds of anions.⁶ When the crystals of **1** were stirred in a tetrahydrofuran (THF)/methanol (MeOH) (1:1, v/v) solution of NaClO_4 (excess), the IR spectra indicated that the typical bands associated with ClO_4^- (~ 1090 cm^{-1}) appeared. As time went on, the intensity of the ClO_4^- band increased, while the intensity of the PF_6^- band (~ 840 cm^{-1}) decreased. After 8 h, no more changes for the band intensity have been observed, indicating that the exchange reaction of PF_6^- by ClO_4^- finished (Figure 5). The PXRD patterns suggest

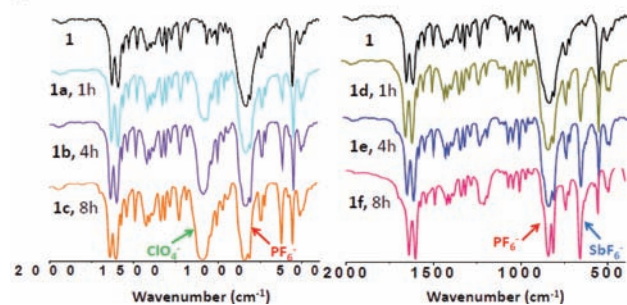


Figure 5. Left: IR spectra of **1** and its anion-exchanged products (PF_6^- by ClO_4^-) obtained after 1 h (**1a**), 4 h (**1b**), and 8 h (**1c**). Right: IR spectra of **1** and its anion-exchanged products (PF_6^- by SbF_6^-) obtained after 1 h (**1d**), 4 h (**1e**), and 8 h (**1f**).

that the skeletal structure of the tube remains intact after anion exchange (Supporting Information). Ion chromatography measurement indicated that 63.26% of the PF_6^- anions in **1** were exchanged by ClO_4^- to result in a mixed-anion compound (**4**).

Besides ClO_4^- , PF_6^- in **1** can also be replaced by SbF_6^- . The crystals of **1** were suspended in a THF/MeOH (1:1, v/v) solution of NH_4SbF_6 and stirred for 8 h; the anion-exchanged product was obtained. The anion-exchange process was monitored by the enhanced intensity at 658 cm^{-1} of the SbF_6^- band, as well as the reduced intensity at 840 cm^{-1} of the PF_6^- band (Figure 5). Again, the ion chromatography analysis suggested that 61.43% of the PF_6^- anions were replaced by SbF_6^- to generate a mixed-anion compound (**5**), and the PXRD patterns confirmed the framework to be intact upon anion exchange (Supporting Information). It is worth noting that anion exchange of **1–3** was found to be highly selective; only the substitution of PF_6^- in **1** by ClO_4^- or SbF_6^- was achieved, whereas ClO_4^- in **2** and SbF_6^- in **3** could not be replaced by PF_6^- or SbF_6^- and ClO_4^- or PF_6^- , respectively,

which is further confirmed by the fact that **1** cannot be regenerated upon the addition of PF_6^- to **4** and **5** under the experimental conditions. Additionally, trigonal-planar NO_3^- was also used to exchange the octahedral PF_6^- in **1**, SbF_6^- in **2**, and the tetrahedral ClO_4^- in **3** under the same experimental conditions, but they did not work. This demonstrates that this anion-exchange process depends on the size and geometry of the anion in relation to the size of the void in the host tube.

The major hurdle in anionic separation is selectivity, that is, the preparation of a host framework that responds to only one kind of specific anion species in the presence of other different potential competitors. As mentioned above, PF_6^- in the tube of **1** can be replaced by both ClO_4^- and SbF_6^- , so we wondered if **1** could be used as a selective anionic acceptor to separate ClO_4^- and SbF_6^- . When the crystals of **1** were stirred in a THF/MeOH (1:1, v/v) solution of equimolar NH_4SbF_6 and NaClO_4 for 6 h, only the characteristic bands of PF_6^- ($\sim 840\text{ cm}^{-1}$) and ClO_4^- (1090 cm^{-1}) were found in the IR spectra; the characteristic band ($\sim 658\text{ cm}^{-1}$) of SbF_6^- , however, was not observed (Supporting Information). The result demonstrates that only ClO_4^- was allowed into the channel to exchange PF_6^- . Therefore, between ClO_4^- and SbF_6^- , ClO_4^- is the preferred anionic species for the host tube of **1**. The PXRD patterns indicate that the structure of **1** is stable during the anion-exchange process (Supporting Information).

We have been exploring the guest-driven luminescent property based on porous MOFs.⁷ As a part of our systematic study on this subject, a luminescent emission spectrum was used to monitor the anion-exchange process. Interestingly, these anions- Ag_2L_2 systems show an interesting anion-responsive photoluminescence. As shown in Figure 6, **1**

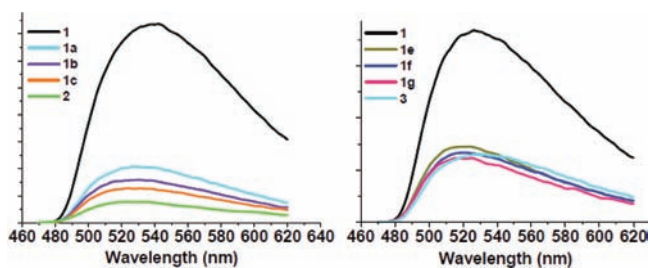


Figure 6. Left: Emission spectra of **1** and **2** and anion-exchanged products based on **1** (PF_6^- by ClO_4^-) at 1 h (**1a**), 4 h (**1b**), and 8 h (**1c**). Right: Emission spectra of **1** and **3** and anion-exchanged products based on **1** (PF_6^- by SbF_6^-) at 1 h (**1d**), 4 h (**1e**), and 8 h (**1f**).

exhibits intense green emission at 527 nm upon excitation at 448 nm, which is of great interest because of an emission characteristic similar to that of a green fluorescent protein of Topaz (T203Y type).⁸ In comparison with the emission of free **L** (528 nm upon excitation at 448 nm; Supporting Information), the emission of **1** should be assigned to the ligand-centered ($n-\pi^*$ or $\pi-\pi^*$) emission because almost identical emission bands are observed. Compared to **1**, **2** and **3** show distinctly different emission properties. The ligand-centered emission intensity in **2** or **3** is dramatically quenched (Figure 6), which is clearly attributed to the different anion inclusions. As expected, the emission intensity of **1** decreased by degrees as the incorporated PF_6^- was gradually replaced by ClO_4^- in **2** and SbF_6^- in **3**, respectively. So, such a metal-organic tube also acts as a luminescent receptor for selective

anion monitoring, which might be of biological, environmental, and industrial interest.

We expect this approach to be viable for the construction of many more new tubular MOFs, and studies toward the preparation of new discrete nanotubes in our laboratory are underway.

■ ASSOCIATED CONTENT

📄 Supporting Information

X-ray crystallographic data in CIF format, syntheses of **L** and **1–3**, TGA and PXRD, spectra, and single-crystal data. This material is available free of charge via the Internet at <http://pubs.acs.org>.

■ AUTHOR INFORMATION

✉ Corresponding Author

*E-mail: yubindong@sdsu.edu.cn.

📝 Notes

The authors declare no competing financial interest.

■ ACKNOWLEDGMENTS

We are grateful for financial support from NSFC (Grant Nos. 91027003 and 21072118), “PCSIRT”, 973 Program (Grant No. 2012CB821705), Shandong Natural Science Foundation (Grant No. JQ200803) and Taishan scholars' construction project special fund.

■ REFERENCES

- (a) Li, J.-R.; Kuppler, R. J.; Zhou, H.-C. *Chem. Rev. Soc.* **2009**, *38*, 1477. (b) Corma, A.; García, H.; Xamena, F. X. L. *Chem. Rev.* **2010**, *110*, 4606. (c) Cui, Y.; Yue, Y.; Qian, G.; Chen, B. *Chem. Rev.* **2011**, *112* (2), 1126–1162.
- (a) Hong, M.-C.; Zhao, Y.-J.; Su, W.-P.; Cao, R.; Fujita, M.; Zhou, Z.-Y.; Chan, A. S. C. *Angew. Chem., Int. Ed.* **2000**, *39*, 2468. (b) Su, C.-Y.; Goforth, A. M.; Smith, M. D.; Pellechia, P. J.; zur Loye, H.-C. *J. Am. Chem. Soc.* **2004**, *126*, 3576. (c) Zhao, B.; Cheng, P.; Dai, Y.; Cheng, C.; Liao, D.-Z.; Yan, S.-P.; Jiang, Z.-H.; Wang, G.-L. *Angew. Chem., Int. Ed.* **2003**, *42*, 934.
- (3) Some typical discrete metal-organic tubes: (a) Pickering, A. L.; Seeber, G.; Long, D. L.; Cronin, L. *Chem. Commun.* **2004**, 1136. (b) Fei, Z.; Zhao, D.; Geldbach, T. J.; Scopelliti, R.; Dyson, P. J.; Antonijevic, S.; Bodenhausen, G. *Angew. Chem., Int. Ed.* **2005**, *44*, 5720. (c) Dong, Y.-B.; Jiang, Y.-Y.; Li, J.; Ma, J.-P.; Liu, F.-L.; Tang, B. *J. Am. Chem. Soc.* **2007**, *129*, 4520. (d) Dai, F.-N.; He, H.-Y.; Sun, D.-F. *J. Am. Chem. Soc.* **2008**, *130*, 14064. (e) Huang, X.-C.; Luo, W.; Shen, Y.-F.; Lin, X.-J.; Li, D. *Chem. Commun.* **2008**, 3995. (f) Luo, T.-T.; Wu, H.-C.; Jao, Y.-C.; Huang, S.-M.; Tseng, T.-W.; Wen, Y.-S.; Lee, G.-H.; Peng, S.-M.; Lu, K.-L. *Angew. Chem., Int. Ed.* **2009**, *48*, 9461.
- (4) Beer, P. D.; Gale, P. A. *Angew. Chem., Int. Ed.* **2001**, *40*, 486.
- (5) Caltagirone, C.; Gale, P. A. *Chem. Soc. Rev.* **2009**, *38*, 520.
- (6) (a) Fei, H.; Rogow, D. L.; Oliver, S. R. *J. Am. Chem. Soc.* **2010**, *132*, 7202. (b) Vyasamudri, S. Y.; Maji, T. K. *Chem. Phys. Lett.* **2009**, *473*, 312. (c) Wang, D.; He, H.; Chen, X.; Feng, S.; Niu, N.; Sun, D. *CrytEngComm* **2010**, *12*, 1041.
- (7) (a) Dong, Y.-B.; Wang, P.; Ma, J.-P.; Zhao, X.-X.; Wang, H.-Y.; Tang, B.; Huang, R.-Q. *J. Am. Chem. Soc.* **2007**, *129*, 4872. (b) Wang, P.; Ma, J.-P.; Dong, Y.-B.; Huang, R.-Q. *J. Am. Chem. Soc.* **2007**, *129*, 10620.
- (8) Zimmer, M. *Chem. Rev.* **2002**, *102*, 759.